

Artificial intelligence-based analysis of body composition in Marfan: skeletal muscle density and psoas muscle index predict aortic enlargement

Nick Lasse Beetz^{1*} , Christoph Maier¹, Seyd Shnayien², Tobias Daniel Trippel^{3,4}, Petra Gehle³, Uli Fehrenbach^{1†} & Dominik Geisel^{1†}

¹Charité—Universitätsmedizin Berlin, corporate member of Freie Universität Berlin and Humboldt-Universität zu Berlin, Department of Radiology, Augustenburger Platz 1, 13353, Berlin, Germany; ²Charité—Universitätsmedizin Berlin, corporate member of Freie Universität Berlin and Humboldt-Universität zu Berlin, Department of Radiology, Hindenburgdamm 30, 12203, Berlin, Germany; ³Charité—Universitätsmedizin Berlin, corporate member of Freie Universität Berlin and Humboldt-Universität zu Berlin, Department of Internal Medicine – Cardiology, Berlin, Germany; ⁴DZHK (German Centre for Cardiovascular Research), partner site Berlin, Germany

Abstract

Background Patients with Marfan syndrome are at risk for aortic enlargement and are routinely monitored by computed tomography (CT) imaging. The purpose of this study is to analyse body composition using artificial intelligence (AI)-based tissue segmentation in patients with Marfan syndrome in order to identify possible predictors of progressive aortic enlargement.

Methods In this study, the body composition of 25 patients aged ≤ 50 years with Marfan syndrome and no prior aortic repair was analysed at the third lumbar vertebra (L3) level from a retrospective dataset using an AI-based software tool (Visage Imaging). All patients underwent electrocardiography-triggered CT of the aorta twice within 2 years for suspected progression of aortic disease, suspected dissection, and/or pre-operative evaluation. Progression of aortic enlargement was defined as an increase in diameter at the aortic sinus or the ascending aorta of at least 2 mm. Patients meeting this definition were assigned to the ‘progressive aortic enlargement’ group (proAE group) and patients with stable diameters to the ‘stable aortic enlargement’ group (staAE group). Statistical analysis was performed using the Mann–Whitney *U* test. Two possible body composition predictors of aortic enlargement—skeletal muscle density (SMD) and psoas muscle index (PMI)—were analysed further using multivariate logistic regression analysis. Aortic enlargement was defined as the dependent variant, whereas PMI, SMD, age, sex, body mass index (BMI), beta blocker medication, and time interval between CT scans were defined as independent variants.

Results There were 13 patients in the proAE group and 12 patients in the staAE group. AI-based automated analysis of body composition at L3 revealed a significantly increased SMD measured in Hounsfield units (HUs) in patients with aortic enlargement (proAE group: 50.0 ± 8.6 HU vs. staAE group: 39.0 ± 15.0 HU; $P = 0.03$). PMI also trended towards higher values in the proAE group (proAE group: 6.8 ± 2.3 vs. staAE group: 5.6 ± 1.3 ; $P = 0.19$). Multivariate logistic regression revealed significant prediction of aortic enlargement for SMD ($P = 0.05$) and PMI ($P = 0.04$).

Conclusions Artificial intelligence-based analysis of body composition at L3 in Marfan patients is feasible and easily available from CT angiography. Analysis of body composition at L3 revealed significantly higher SMD in patients with progressive aortic enlargement. PMI and SMD significantly predicted aortic enlargement in these patients. Using body composition as a predictor of progressive aortic enlargement may contribute information for risk stratification regarding follow-up intervals and the need for aortic repair.

Keywords Marfan syndrome; Aortic enlargement; Body composition; Sarcopenia

Received: 16 February 2021; Revised: 11 May 2021; Accepted: 21 May 2021

*Correspondence to: Dr Nick Lasse Beetz, MD, Charité—Universitätsmedizin Berlin, corporate member of Freie Universität Berlin and Humboldt-Universität zu Berlin, Department of Radiology, Augustenburger Platz 1, 13353 Berlin, Germany. Phone: +49-30-450657278, Fax: +49-30-4507527911, Email: nick-lasse.beetz@charite.de
 †Uli Fehrenbach and Dominik Geisel contributed equally to this work and share the last authorship.

Introduction

The Marfan syndrome is an inherited connective tissue disorder with an estimated incidence of 2–3 per 10 000 individuals. Its phenotype is characterized by cardiovascular, musculoskeletal, and ocular abnormalities.¹ Several mutations for the classical Marfan syndrome have been described and they frequently involve the fibrillin-1 gene (*FBNI*).^{2,3} Major criteria for the diagnosis of Marfan syndrome according to the Ghent nosology include dilation of the aortic root, aortic dissection, ectopia lentis, characteristic skeletal abnormalities, and certain genetic mutations.⁴

Untreated patients with Marfan syndrome are at risk for aortic dissection, aortic rupture, primary cardiomyopathy, and heart failure due to mitral or aortic valve regurgitation. In the past, mean life expectancy was as low as 32 years.^{5,6} As cardiovascular manifestations are the main cause of morbidity and mortality, complete aortic imaging in patients with suspected Marfan syndrome and related disorders is recommended.^{7,8} Monitoring patients at risk for aortic dilatation and the advent of surgical repair for aortic aneurysms have greatly improved long-term survival in Marfan syndrome.⁹

For initial assessment of aortic diameter, patients with Marfan syndrome usually undergo echocardiography, as recommended by international guidelines.¹⁰ To avoid underestimation of aortic enlargement, when determined by echocardiography, it is recommended to supplement the initial examination by additional computed tomography (CT) or magnetic resonance imaging (MRI) of the aorta.⁸ While yearly follow-up imaging is generally performed with echocardiography, CT or MRI angiography is appropriate if initial sonographic assessment underestimated cross-sectional aortic diameter, dissection is clinically suspected, or surgical aortic repair is intended.^{11,12}

Typical musculoskeletal findings in patients with Marfan syndrome are arachnodactyly, pectus deformity, scoliosis, acetabular protrusion, and disproportionately long extremities.¹³ Other abnormalities including reduced bone mineral density, reduced muscle mass, and muscle weakness have been described and might influence body composition of affected patients.^{14,15}

Evaluation of body composition as a possible predictor of cardiovascular disease is well established. For example, abdominal obesity has been shown to be highly predictive of coronary heart disease, and the psoas muscle area at the level of the third lumbar vertebra (L3) appears to predict outcome in patients undergoing transcatheter aortic valve implantation.^{16,17} CT allows straightforward analysis of body composition and quantification of sarcopenia.^{18,19} As manual segmentation of CT datasets is time consuming,

earlier studies investigating body composition analysis have often been performed in small patient populations. Artificial intelligence-based automated tissue segmentation can dramatically decrease post-processing time of these datasets.²⁰

This study aims to retrospectively analyse the body composition of patients with Marfan syndrome using artificial intelligence (AI)-based automated tissue segmentation and to identify possible features of body composition that might predict progression of aortic enlargement.

Materials and methods

Study design

In this single-centre study, we analysed body composition and aortic diameters in a retrospective dataset of patients who underwent CT imaging of the entire aorta twice within 2 years. The study was approved by the institutional review board.

Patient cohort and patient characteristics

All patients diagnosed with Marfan syndrome at the outpatient Marfan Center of the Charité University Hospital Berlin who were referred to the Department of Radiology between 2018 and 2020 were included in this study, if they underwent electrocardiography-triggered CT angiography of the aorta twice within 2 years due to suspected progression of aortic enlargement, suspected aortic dissection, or pre-operative evaluation for surgical repair or replacement. Exclusion criteria were prior surgical or interventional aortic repair and patient age greater than 50 years as aortic enlargement in older patients might have causes other than Marfan syndrome.

Progression of aortic enlargement was defined as an increase in the diameter of the aortic sinus or the ascending aorta of at least 2 mm within 2 years. Patients with progressive aortic enlargement were assigned to the 'progressive aortic enlargement' group (proAE group), whereas patients without progressive aortic enlargement were assigned to the 'stable aortic enlargement' group (staAE group).

Image acquisition and aortic diameter measurement

All patients referred to the Department of Radiology were examined in the same single-source 256-row CT scanner

(Revolution CT, General Electric, Milwaukee, USA). After intravenous bolus injection of iodinated contrast medium, an axial ECG-triggered whole-heart scan including the aortic root was performed, immediately followed by a helical scan of the entire aorta. Adequate opacification of the aorta was ensured by bolus tracking with SmartPrep (General Electric, Milwaukee, USA).

Aortic diameters were determined from double oblique multiplanar reconstructions perpendicular to the course of the vessel using Merlin viewer (Phoenix-PACS GmbH, Freiburg im Breisgau, Germany).

Measurements were performed at the levels of the aortic sinus and the largest diameter of the ascending aorta (proximal to the branching of the brachiocephalic trunk). Aortic diameter was consistently measured from outer edge to outer edge during serial follow-up imaging.

Body composition analysis

For analysis of body composition, we used an AI-based automated software tool based on a convolutional neural network, U-net, developed for image segmentation (Visage version 7.1., Visage Imaging GmbH, Berlin, Germany). The network consists of nine blocks: four downsampling blocks, four upsampling blocks, and one in between. The training data consisted of 200 axial CT images of the L3 level, and augmentation was applied during training to improve generalization of the network. Tissue was separated into psoas muscle, skeletal muscle, visceral fat, and subcutaneous fat and coded with different colours. Other tissues, such as kidney, liver, spleen, intestine, and pancreas, were not segmented. False tissue segmentation occurred in a few cases, for example, when hypodense stool in the intestine was misinterpreted as body fat, and was manually corrected. The area in square centimetres (cm²) and density in Hounsfield unit (HU) of each segmented tissue class were automatically calculated by the software. The following parameters were derived from L3 body composition analysis: mean density (in HU) of skeletal muscle including the psoas muscle (SMD), and areas (in cm²) of skeletal muscle, visceral adipose tissue (VAT), and subcutaneous adipose tissue (SAT). The psoas muscle index (PMI) was calculated using the following formula: psoas muscle area (cm²)/body surface area (m²). Two possible body composition predictors of aortic enlargement—SMD and PMI—were analysed further using multivariate logistic regression analysis. Aortic enlargement was defined as a dependent variant, whereas PMI, SMD, age, sex, body mass index (BMI), beta blocker medication, and time interval between CT scans were defined as independent variants. An example of AI-based automated analysis of L3 body composition is shown in *Figure 1*.

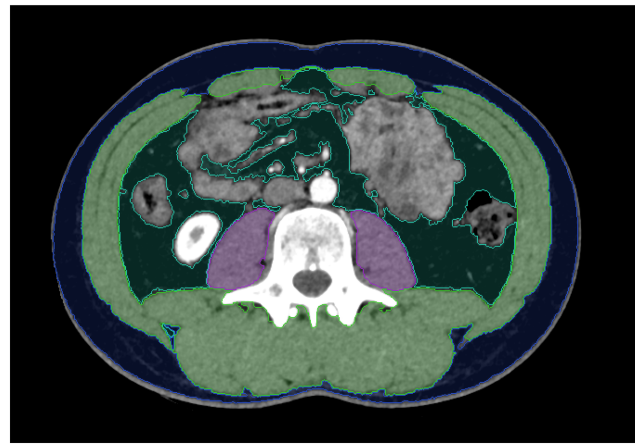


Figure 1 Example of artificial intelligence-based automated analysis of L3 body composition in an 18-year-old male patient with diagnosed Marfan syndrome. Each segmented tissue is coded with a different colour: psoas muscle = purple, skeletal muscle (except psoas muscle) = green, visceral fat = dark green, blue = subcutaneous fat. Tissue density and area were automatically calculated using Visage version 7.1.

Statistical analysis

The Shapiro–Wilk test was used to test for normal distribution. Statistical significance of differences between the two groups was evaluated using the Mann–Whitney *U* test, and a *P* value ≤ 0.05 was considered to indicate a significant difference. For prediction of aortic enlargement, multivariate logistic regression was performed. All data analyses were performed using IBM SPSS Statistics version 27 (IBM, Armonk, New York, USA).

Results

Baseline data

A total of 25 patients were included in this study. There were no significant differences regarding possible confounders including age (proAE group: mean 32 ± 8 years; staAE group: mean 37 ± 9 years; *P* = 0.10), time interval between the two follow-up CT angiographies (proAE group: mean 559 ± 240 ; staAE group: mean 482 ± 234 days; *P* = 0.42) and sex (proAE group: 5 female and 8 male patients; staAE group: 5 female and 7 male patients; *P* = 0.88). Except for one patient per group, all patients were on medication including a renin–angiotensin system antagonist or beta blocker. The patients' baseline characteristics are summarized in *Table 1*. The mean dose-length product was $447.7 \text{ mGy} \cdot \text{cm}$ in the first and $553.4 \text{ mGy} \cdot \text{cm}$ in the second CT angiography.

Table 1 Demographic characteristics and time interval between the two follow-up CT scans analysed in this retrospective study

	Total (mean ± SD)	proAE (mean ± SD)	staAE (mean ± SD)	P value
Number of patients	25	13	12	
Age (years)	35 ± 9	32 ± 8.37	± 9	0.10
Body height (cm)	187 ± 13	189 ± 11	185 ± 14	0.54
BMI (kg/m ²)	24 ± 6	23 ± 4	25 ± 7	0.38
Sex (♂/♀)	15/10	8/5	7/5	0.88
Interval between CT scans (days)	522 ± 235	559 ± 240	482 ± 234 days	0.42

Data are provided for the total population and the two subgroups. proAE group = group with progressive aortic enlargement; staAE group = group with stable aortic enlargement. BMI, body mass index; CT, computed tomography.

Diameters of aortic sinus and ascending aorta

In the first CT examination, the mean diameter of the aortic sinus was 44 ± 3.9 mm in the proAE group (with progression of aortic enlargement) and 44 ± 4.4 mm in the staAE group (without progression of aortic enlargement). The mean diameter of the ascending aorta was 34 ± 6.4 mm in the proAE group and 36 ± 8.8 in the staAE group. There was no statistically significant difference in the initial diameters measured in first CT angiography between the proAE group and the staAE group (aortic sinus: $P = 0.86$; and ascending aorta: $P = 0.45$).

The second CT angiography yielded a mean diameter of the aortic sinus of 46 ± 3.7 mm and a mean diameter of the ascending aorta of 35 ± 7.5 mm in the proAE group, whereas in the staAE group, the mean diameter of the aortic sinus was 45 ± 5.1 mm, and the mean diameter of the ascending aorta was 36 ± 8.8 mm.

Body composition

Patients with progressive aortic enlargement had a higher SMD (proAE group: SMD = 50.0 ± 8.6 HU vs. staAE group: SMD = 39.0 ± 15.0 HU; $P = 0.03$). The PMI also trended towards higher values in the proAE group (proAE group: PMI = 6.8 ± 2.3 vs. staAE group: PMI = 5.6 ± 1.3; $P = 0.19$).

No differences between the two groups regarding other parameters of body composition such as VAT (proAE group: 85.1 ± 59.8 mm²; staAE group: 104.3 ± 88.0 mm²; $P = 0.53$) and SAT (proAE group: 125.6 ± 57.3 mm²; staAE group: 182.6 ± 140 mm²; $P = 0.19$) were found. All results are compiled in *Figures 1 and 2*.

Multivariate logistic regression with aortic enlargement as dependent variant was performed for PMI and SMD, each combined with other independent variants including age, sex, BMI, beta blocker medication, and time interval between the two CT angiographies. Significant predictors of

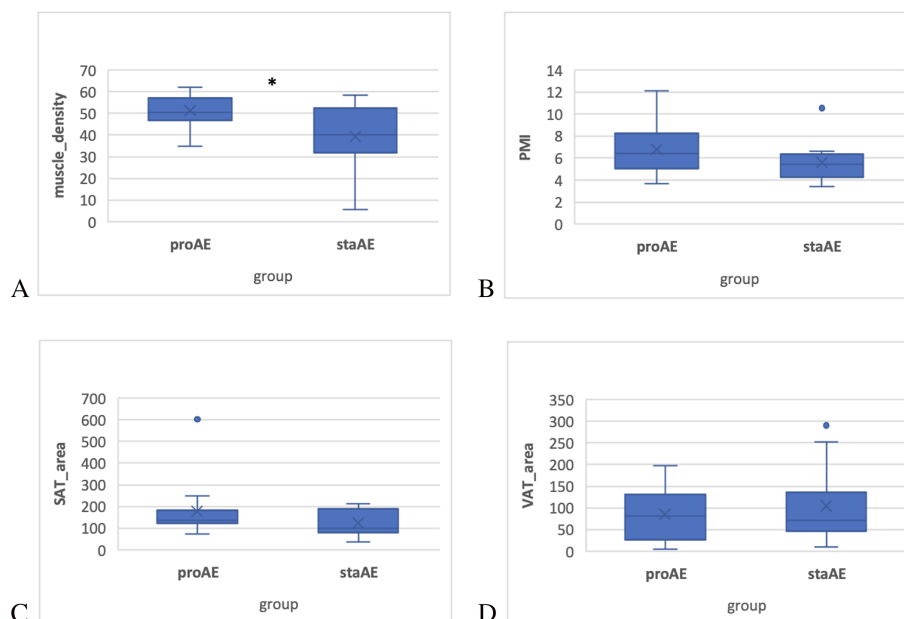


Figure 2 Box plots visualizing analysis of AI-based automated L3 body composition in Marfan patients: (A) muscle density (in HU), (B) PMI (in cm²/m²), (C) SAT area, and (D) VAT area. AI, artificial intelligence; HU, Hounsfield unit; L3, third lumbar vertebra; PMI, psoas muscle index; SAT, subcutaneous adipose tissue; VAT, visceral adipose tissue. An asterisk (*) indicates statistically significant results ($P \leq 0.05$).

Table 2 Results of multivariate logistic regression analysis for possible body composition predictors of aortic enlargement as dependent variable

Aortic enlargement	Coef.	SEM	t value	P value (95% conf interval)	Sig
(A)					
Sex	-2.119	1.572	-1.35	0.178	0.962
Age	-0.087	0.072	-1.21	0.226	0.054
BMI	-0.391	0.26	-1.50	0.133	0.118
Beta blockers	0.619	1.739	0.36	0.722	4.027
Time interval	0.004	0.003	1.08	0.279	0.01
PMI	1.766	0.861	2.05	0.04	3.455
Constant	1.219	5.062	0.24	0.81	11.14
(B)					
Sex	-0.231	1.135	-0.20	0.839	1.994
Age	-0.09	0.069	-1.30	0.194	0.046
BMI	0.179	0.155	1.15	0.25	0.483
Beta blockers	-1.173	1.37	-0.86	0.392	1.513
Time interval	0.001	0.002	0.27	0.784	0.005
SMD	0.133	0.067	1.99	0.046	0.264
Constant	-7.161	6.121	-1.17	0.242	4.835

(A) PMI significantly predicts progressive aortic enlargement in patients with Marfan syndrome, whereas other independent variables such as sex, age, BMI, medications including beta blockers, and time interval between the two CT scans analysed do not. (B) SMD significantly predicts progressive aortic enlargement in patients with Marfan syndrome, whereas other independent variables such as gender, age, BMI, medications including beta blockers, and time interval between the two CT scans do not.

BMI, body mass index; Coef., coefficient; Conf. interval, confidence interval; PMI, psoas muscle index; SEM, standard error of the mean; sig, significance; SMD, skeletal muscle density; time interval, time interval between the two computed tomography examinations analysed.

* $P < .05$

progressive aortic enlargement were SMD ($P = 0.05$) and PMI ($P = 0.04$). The results are compiled in *Table 2*.

Discussion

In this study, we analysed the body composition of patients with Marfan syndrome from a retrospective dataset of patients who underwent CT angiography of the aorta twice within 2 years. The cohort was divided into two groups: the proAE group with progressive aortic enlargement and the staAE group with stable aortic diameters. After excluding possible confounders such as time between the two examinations and patient characteristics like age, height, and sex, we compared the two groups regarding their body composition. Progressive aortic enlargement was associated with a significantly higher overall SMD in comparison with patients with stable diameters of the aortic sinus and ascending aorta. Additionally, SMD and PMI were found to significantly predict aortic enlargement in patients with Marfan syndrome.

According to the revised Ghent nosology for the Marfan syndrome, enlargement of the aortic root is a major criterion for establishing the diagnosis and is associated with a high risk for aortic dissection and hence cardiovascular mortality.^{2,4,21} As a result of improved monitoring including follow-up imaging and improved surgical and interventional repair techniques available today, patients with Marfan syndrome have near-normal life expectancy if treated in experienced and specialized centres.^{22,23} Patients with progression of aortic enlargement are at risk, and aortic repair is usually recommended.^{24,25}

Segmentation of a single-slice axial CT image at the L3 level is an established reference method for body composition analysis and has shown to be a useful indicator for prognosis and risk stratification in several diseases, particularly cardiovascular and malignant conditions.^{26–28} Both sarcopenia and sarcopenic obesity are risk factors in cardiovascular disease but are also associated with unfavourable outcomes in malignancies and with prolonged postoperative recovery.^{29–32} However, the influence of body composition in Marfan syndrome has not been evaluated before.

Skeletal muscle density is influenced by an individual's activity level and correlates with physical fitness.^{33,34} In general, patients with Marfan syndrome and relevant enlargement of the aorta are advised to avoid strenuous activity, especially contact sports and isometric exercises like weightlifting and push-ups, as acute dissection and progressive aortic enlargement of the great vessels are feared complications.³⁵ In our study, patients with progressive aortic enlargement had a significantly higher SMD, which indicates a higher level of physical activity and fitness. While the PMI also trended to be higher in these patients, the difference did not reach statistical significance in our small study population. Our results are further corroborated by a multivariate regression analysis identifying SMD and PMI—two parameters of body composition representing muscle tissue—as significant predictors of aortic enlargement.

Analysis of body composition at L3 allows objective assessment of physical activity in patients examined by CT imaging.^{36,37} We are the first to show that AI-based automated quantification and qualification of L3 body composition in patients with Marfan syndrome who underwent

CT angiography for follow-up or pre-operative evaluation is feasible and may improve risk stratification regarding further lifestyle and treatment recommendations.

As CT angiography of the entire aorta is routinely performed and recommended for the monitoring of patients with Marfan syndrome, extraction of possible predictors of progressive aortic enlargement might also be relevant for follow-up imaging: patients with lower SMD and lower PMI might have a lower risk of progressive aortic enlargement, and therefore, a more conservative approach and less frequent follow-up CT angiographies might be justified. Longer intervals between CT angiographies are desirable to reduce radiation exposure in this group of often young patients.³⁸ Moreover, morbidity related to side effects of contrast media, such as allergic reactions and kidney failure, may be reduced.³⁹

Limitations

Our study is limited by the use of a retrospective dataset and the relatively small cohort. As many patients with Marfan syndrome undergo aortic repair at an early age, there might have been a selection bias towards patients with less severe disease. Finally, muscle density on CT primarily reflects muscle structure and physical fitness but may be influenced by the amount of contrast medium uptake.

References

- Judge DP, Dietz HC. Marfan's syndrome. *Lancet (London, England)* 2005;**366**: 1965–1976.
- Cook JR, Carta L, Galatioto J, Ramirez F. Cardiovascular manifestations in Marfan syndrome and related diseases; multiple genes causing similar phenotypes. *Clin Genet* 2015;**87**:11–20.
- Akhurst RJ. TGF β signaling in health and disease. *Nat Genet* 2004;**36**:790–792.
- Loeys BL, Dietz HC, Braverman AC, Callewaert BL, De Backer J, Devereux RB, et al. The revised Ghent nosology for the Marfan syndrome. *J Med Genet* 2010;**47**:476–485.
- Nienaber CA, Von Kodolitsch Y. Therapeutic management of patients with Marfan syndrome: focus on cardiovascular involvement. *Cardiol Rev* 1999;**7**:332–341.
- Pyeritz RE. Marfan syndrome: improved clinical history results in expanded natural history. *Genet Med* 2019;**21**:1683–1690.
- Baumgartner H, De Backer J, Babu-Narayan SV, Budts W, Chessa M, Diller GP, et al. 2020 ESC guidelines for the management of adult congenital heart disease. *Eur Heart J* 2020;**42**:563–645.
- Hiratzka LF, Bakris GL, Beckman JA, Bersin RM, Carr VF, Casey DE Jr, et al. 2010 ACCF/AHA/AATS/ACR/ASA/SCA/SCAI/SIR/STS/SVM guidelines for the diagnosis and management of patients with thoracic aortic disease: a report of the American College of Cardiology Foundation/American Heart Association Task Force on Practice Guidelines, American Association for Thoracic Surgery, American College of Radiology, American Stroke Association, Society of Cardiovascular Anesthesiologists, Society for Cardiovascular Angiography and Interventions, Society of Interventional Radiology, Society of Thoracic Surgeons, and Society for Vascular Medicine. *Circulation* 2010;**121**:e266–e369.
- Finkbohner R, Johnston D, Crawford ES, Coselli J, Milewicz DM. Marfan syndrome: long-term survival and complications after aortic aneurysm repair. *Circulation* 1995;**91**:728–733.
- Mokashi SA, Svensson LG. Guidelines for the management of thoracic aortic disease in 2017. *Gen Thorac Cardiovasc Surg* 2019;**67**:59–65.
- Chu LC, Johnson PT, Dietz HC, Fishman EK. CT angiographic evaluation of genetic vascular disease: role in detection, staging, and management of complex vascular pathologic conditions. *AJR Am J Roentgenol* 2014;**202**:1120–1129.
- Bons LR, Duijnhouwer AL, Boccacini S, van den Hoven AT, van der Vlugt MJ, Chelu RG, et al. Intermodality variation of aortic dimensions: how, where and when to measure the ascending aorta. *Int J Cardiol* 2019;**276**:230–235.
- Meester JAN, Verstraeten A, Schepers D, Alaerts M, Van Laer L, Loeys BL. Differences in manifestations of Marfan syndrome, Ehlers–Danlos syndrome, and Loeys–Dietz syndrome. *Ann Cardiothorac Surg* 2017;**6**: 582–594.
- Jones KB, Sponseller PD, Erkula G, Sakai L, Ramirez F, Dietz HC 3rd, et al. Symposium

Conclusion

Artificial intelligence-based analysis of L3 body composition is feasible in Marfan patients and easily available from CT angiography. SMD and PMI are indicators of physical activity and training. An increase in these parameters during follow-up of Marfan syndrome significantly predicts the progression of aortic enlargement. Using body composition as a predictor of progressive aortic enlargement may contribute information to risk stratification regarding follow-up intervals and the need for surgical or interventional aortic repair.

Acknowledgements

The authors of this manuscript certify that they comply with the ethical guidelines for authorship and publishing in the *Journal of Cachexia, Sarcopenia and Muscle*.⁴⁰

Conflict of interest

Uli Fehrenbach reports honoraria and travel expenses for scientific meetings (outside of submitted work) from Bayer, Siemens, and General Electrics. Nick Lasse Beetz, Christoph Maier, Seyd Shnayien, Tobias Daniel Trippel, Petra Gehle, and Dominik Geisel declare that they have no conflict of interest.

- on the musculoskeletal aspects of Marfan syndrome: meeting report and state of the science. *J Orthop Res* 2007;**25**:413–422.
15. von Kodolitsch Y, Demolder A, Girdauskas E, Kaemmerer H, Kornhuber K, Muino Mosquera L, et al. Features of Marfan syndrome not listed in the Ghent nosology—the dark side of the disease. *Expert Rev Cardiovasc Ther* 2019;**17**:883–915.
 16. Canoy D, Boekholdt SM, Wareham N, Luben R, Welch A, Bingham S, et al. Body fat distribution and risk of coronary heart disease in men and women in the European Prospective Investigation Into Cancer and Nutrition in Norfolk cohort: a population-based prospective study. *Circulation* 2007;**116**:2933–2943.
 17. Kofler M, Reinstadler SJ, Mayr A, Stastny L, Reindl M, Dumfarth J, et al. Prognostic implications of psoas muscle area in patients undergoing transcatheter aortic valve implantation. *Eur J Cardiothorac Surg* 2019;**55**:210–216.
 18. Gibson DJ, Burden ST, Strauss BJ, Todd C, Lal S. The role of computed tomography in evaluating body composition and the influence of reduced muscle mass on clinical outcome in abdominal malignancy: a systematic review. *Eur J Clin Nutr* 2015;**69**:1079–1086.
 19. Faron A, Sprinkart AM, Kuetting DLR, Feisst A, Isaak M, Endler C, et al. Body composition analysis using CT and MRI: intra-individual intermodal comparison of muscle mass and myosteatosis. *Sci Rep* 2020;**10**:11765.
 20. Wang B, Torriani M. Artificial intelligence in the evaluation of body composition. *Semin Musculoskelet Radiol* 2020;**24**:30–37.
 21. Desai MY, Kalahasti V, Hutt Centeno E, Chen K, Alashi A, Rivas CG, et al. Adult patients with Marfan syndrome and ascending aortic surgery. *J Am Coll Cardiol* 2019;**73**:733–734.
 22. Conway AM, Qato K, Anand G, Mondry L, Giangola G, Carroccio A. Endovascular abdominal aortic aneurysm repair in patients with Marfan syndrome. *Vascular* 2020;**28**:48–52.
 23. Gott VL, Laschinger JC, Cameron DE, Dietz HC, Greene PS, Gillinov AM, et al. The Marfan syndrome and the cardiovascular surgeon. *Eur J Cardiothorac Surg* 1996;**10**:149–158.
 24. Jondeau G, Detaint D, Tubach F, Arnoult F, Milleron O, Raoux F, et al. Aortic event rate in the Marfan population: a cohort study. *Circulation* 2012;**125**:226–232.
 25. Erbel R, Aboyans V, Boileau C, Bossone E, Bartolomeo RD, Eggebrecht H, et al. 2014 ESC guidelines on the diagnosis and treatment of aortic diseases: document covering acute and chronic aortic diseases of the thoracic and abdominal aorta of the adult. The Task Force for the Diagnosis and Treatment of Aortic Diseases of the European Society of Cardiology (ESC). *Eur Heart J* 2014;**35**:2873–2926.
 26. Cespedes Feliciano EM, Popuri K, Cobzas D, Baracos VE, Beg MF, Khan AD, et al. Evaluation of automated computed tomography segmentation to assess body composition and mortality associations in cancer patients. *J Cachexia Sarcopenia Muscle* 2020;**11**:1258–1269.
 27. Institute of Medicine Committee on Military Nutrition Research. In Carlson-Newberry SJ, Costello RB, eds. *Emerging Technologies for Nutrition Research: Potential for Assessing Military Performance Capability*. Washington (DC): National Academies Press (US). Copyright 1997 by the National Academy of Sciences. All rights reserved; 1997.
 28. Scherbakov N, Pietrock C, Sandek A, Ebner N, Valentova M, Springer J, et al. Body weight changes and incidence of cachexia after stroke. *J Cachexia Sarcopenia Muscle* 2019;**10**:611–620.
 29. Ratnayake CB, Loveday BP, Shrikhande SV, Windsor JA, Pandanaboyana S. Impact of preoperative sarcopenia on postoperative outcomes following pancreatic resection: a systematic review and meta-analysis. *Pancreatology* 2018;**18**:996–1004.
 30. Britton KA, Massaro JM, Murabito JM, Kreger BE, Hoffmann U, Fox CS. Body fat distribution, incident cardiovascular disease, cancer, and all-cause mortality. *J Am Coll Cardiol* 2013;**62**:921–925.
 31. Williams GR, Muss HB, Shachar SS. Cachexia in patients with cancer. *Lancet Oncol* 2016;**17**:e220.
 32. Weerink LBM, van der Hoorn A, van Leeuwen BL, de Bock GH. Low skeletal muscle mass and postoperative morbidity in surgical oncology: a systematic review and meta-analysis. *J Cachexia Sarcopenia Muscle* 2020;**11**:636–649.
 33. Hsu KJ, Liao CD, Tsai MW, Chen CN. Effects of exercise and nutritional intervention on body composition, metabolic health, and physical performance in adults with sarcopenic obesity: a meta-analysis. *Nutrients* 2019;**11**:2163.
 34. Evans WJ, Morley JE, Argilés J, Bales C, Baracos V, Guttridge D, et al. Cachexia: a new definition. *Clin Nutr* 2008;**27**:793–799.
 35. Maron BJ, Chaitman BR, Ackerman MJ, Bayés de Luna A, Corrado D, Crosson JE, et al. Recommendations for physical activity and recreational sports participation for young patients with genetic cardiovascular diseases. *Circulation* 2004;**109**:2807–2816.
 36. Mourtzakis M, Prado CM, Lieffers JR, Reiman T, McCargar LJ, Baracos VE. A practical and precise approach to quantification of body composition in cancer patients using computed tomography images acquired during routine care. *Appl Physiol Nutr Metab* 2008;**33**:997–1006.
 37. Fearon K, Strasser F, Anker SD, Bosaeus I, Bruera E, Fainsinger RL, et al. Definition and classification of cancer cachexia: an international consensus. *Lancet Oncol* 2011;**12**:489–495.
 38. Vaiserman A, Koliada A, Zabuga O, Socol Y. Health impacts of low-dose ionizing radiation: current scientific debates and regulatory issues. *Dose Response* 2018;**16**:1559325818796331.
 39. Lightfoot CB, Abraham RJ, Mammen T, Abdolell M, Kapur S, Abraham RJ. Survey of radiologists' knowledge regarding the management of severe contrast material-induced allergic reactions. *Radiology* 2009;**251**:691–696.
 40. von Haehling S, Morley JE, Coats AJS, Anker SD. Ethical guidelines for publishing in the *Journal of Cachexia, Sarcopenia and Muscle*: update 2019. *J Cachexia Sarcopenia Muscle* 2019;**10**:1143–1145.